# Computational exploration of the copper(I)-catalyzed conversion of hydrazones to dihalogenated vinyldiazene derivatives

Ulviyya Askerova<sup>[d]</sup>, Yusif Abdullayev\*<sup>[a,b,c]</sup>, Namiq Shikhaliyev<sup>[d]</sup>, Abel Maharramov<sup>[d]</sup> Valentine G. Nenajdenko<sup>[e]</sup>, Jochen Autschbach<sup>[f]</sup>

- [a] Department of Chemical Engineering, Baku Engineering University, Hasan Aliyev str. 120, Baku, Absheron, AZ0101, Azerbaijan. Email: <a href="mailto:yabdullayev@beu.edu.az">yabdullayev@beu.edu.az</a>
- [b] Institute of Petrochemical Processes, Azerbaijan National Academy of Sciences, Baku AZ1025, Azerbaijan
- [c] Department of Chemistry, Sumgait State University, 43<sup>th</sup> district, Baku str. 1, AZ5008, Sumgait, Azerbaijan
- [d] Organic Chemistry Department, Baku State University, Z. Xalilov str. 23, Az1148, Baku, Azerbaijan
- [e] Department of Chemistry, M. V. Lomonosov Moscow State University, Leninskie Gory 1, Moscow 119991, Russia
- [f] Department of Chemistry, University at Buffalo, State University of New York, Buffalo, New York 14260-3000, United States.

**Keywords:** copper, catalyst, DFT, vinyldiazene, ligand, energy span model

**Abstract:** This computational study explores the copper (I) chloride catalyzed synthesis of (E)-1-(2,2-dichloro-1-phenylvinyl)-2-phenyldiazene (**2CI-VD**) from readily available hydrazone derivative and carbon tetrachloride (CCI<sub>4</sub>). **2CI-VD** has been extensively utilized to synthesize variety of heterocyclic organic compounds in mild conditions. The present computational investigations primarily focus on understanding the role of copper (I) and  $N^1, N^2, N^2$ -tetramethylethane-1,2-diamine (TMEDA) in this reaction, TMEDA often being considered a proton scavenger by experimentalists. Considering TMEDA as a ligand significantly alter the energy barrier. In fact, it is only 8.3 kcal/mol bigger compared to the ligand-free (LF) route for the removal of a chlorine atom to form the radical  $\cdot$ CCl<sub>3</sub> but the next steps are almost barrierless. This intermediate then participates in attacking the electrophilic carbon in the hydrazone. Crucially, the study reveals that the overall potential energy surface is thermodynamically favorable, and the theoretical turnover frequency (TOF) value is remarkably higher in the case of Cu(I)-TMEDA complex catalyzed pathway.

#### 1. Introduction

Vinyldiazene (VD) derivatives are extensively used precursors for the construction of versatile value-added organic substances such as thiazolines, pyrrols, pyrazole N-oxides, pyrazols, triazols, triazols, pyrazol-1(5H)-ones, and 4,5-dihydrothiophenes. (Scheme 1)

**Scheme 1.** Product distribution from vinyldiazenes conversion.

Pyridazine derivatives are frequently utilized scaffolds in medicinal chemistry. 8-11 A tedious multistep procedure was used to synthesize pyridazine moieties. 12 The utilization of halogenated VDs is more advantageous because functionalized pyridazine structures were synthesized quantitatively in a single step at room temperature. 13,14 VD is a hetero-diene with boosted reactivity because of the strong electron-withdrawing feature of the -N=N- group compared to homo-diene systems. Some of us previously synthesized halogenated VD systems, which bear geminal chlorine atoms in the edge vinylic position according to the following reaction scheme to increase reactivity for the straightforward design of several heterocyclic compounds. 15 Synthesis of (E)-1-(2,2-dichloro-1-phenylvinyl)-2-phenyldiazene (2Cl-VD) from 1-benzylidene-2-phenylhydrazine proceeded according to Scheme 2.

**Scheme 2.** The reaction considered in the quantum chemical calculations.

The addition of chlorine substituents to VDs opens up new opportunities to build diverse heterocyclic compounds and other substituted VD derivatives. For example, treatment of malononitrile with **2Cl-VD** yielded pyridazine nitrile derivatives, room temperature reaction between **2Cl-VD** resulted in pyridazin-3(2H)-ones formation, chlorine atoms were replaced with aril groups via Suzuki reaction, and several other functionalization of **2Cl-VD** can be conducted. Treatment of **2Cl-VD** with NaN<sub>3</sub> at room temperature followed the formation of triazole derivatives. Previous experimental studies showed that with the utilized procedure (Scheme 2), several dihalogens or hetero-groups can be introduced at the edge vinylic position via replacing CCl<sub>4</sub> with other halogen derivatives such as CCl<sub>3</sub>CO<sub>2</sub>Et, CF<sub>3</sub>CCl<sub>3</sub>, CF<sub>3</sub>CBr<sub>3</sub>, CCl<sub>3</sub>Br, CBr<sub>4</sub>, and CCl<sub>3</sub>CN. To

Despite the economical and efficient transformations of **2CI-VD** synthon into versatile heterocyclic organic compounds, as stated above, the **2CI-VD** synthesis reaction mechanism has so far not been

investigated theoretically, even though calculations are frequently applied to scrutinize reaction mechanisms. <sup>18-25</sup> TMEDA and other related diamine species have been frequently exploited previously as ligands for stabilizing copper complexes. <sup>26,27</sup> Lumb *et al.* studied copper (I) and some diamine (N,N'-ditert-butylethylenediamine, p-(N,N-dimethylamino)pyridine, etc.) ligands containing homogeneous catalytic systems for selective aerobic oxidation of alcohols to aldehydes. <sup>28-30</sup> As a bidentate amine ligand, TMEDA has also been used in organolithium chemistry. <sup>31</sup>

Here, we focused on identifying the catalytic effects of the TMEDA/CuCl complex in the reaction shown in Scheme 2 through quantum chemical calculations, which had been previously investigated experimentally in detail.<sup>15</sup>

## 2. Computational details.

The Gaussian 16 program <sup>32</sup> was utilized in all calculations. The reaction species such as reactants, products, intermediates, and transition state structures were optimized with Kohn-Sham Density Functional Theory (KS-DFT), using the B3LYP functional<sup>33</sup> with D3BJ dispersion corrections.<sup>34</sup> The 6-311G(d,p) basis set was used for H, C, N, and Cl atoms. def2-TZVP basis set were used for Cu since it is widely utilized for 3d metal atoms.<sup>35,36</sup>

Due to the paramagnetic nature of Cu(II) species (Cu<sup>2+</sup> and ·CCl<sub>3</sub> may result in forming two unpaired electrons in the structures), we also monitored the Gibbs energies concerning the triplet spin states of the relevant species. Our computational observations indicate that structures with triplet spin state generally exhibit energy levels that are predominantly higher than those of singlet species. Singlet/triplet state instability was observed only in the final stage of the mechanism. The energy of I3-Ltns singlet state intermediate is initially quite higher than the corresponding triplet state I3-L-tns-TRIP structure due to potential delocalization of double bonds (C=C-N=N). Further stability analysis of the singlet stationary state (I3-L-tns) revealed the RHF (Restricted Hartree-Fock) → UHF (Unrestricted Hartree-Fock) instability. The broken symmetry approach was used according to the previous study<sup>37</sup> for wavefunction stabilization, and eventually, we achieve to stabilize the related energy for the I3-L-tns intermediate (See Figure 2, and ESI, Figure S2 for molecular orbital analysis). Solvent effects were studied via a self-consistent reaction field (SCRF) and default polarizable continuum model (PCM) with a dielectric constant for DMSO ( $\varepsilon$ = 46.826).<sup>38</sup> Minima (no imaginary frequency), transition states (one imaginary frequency), and free energies (including entropy contributions from rotations, vibrations, and translation) were determined via analytic frequency calculations. Gibbs energies and related data are given for a temperature of 298.15 K because of experimentally applied procedures. Intrinsic reaction coordinate (IRC) searches were applied to connect the transition state (TS) and intermediate/product structures.<sup>39</sup> Optimized geometries (in xyz format), total energies, Gibbs energies, and enthalpies of all structures are given in the electronic supporting information (ESI).

#### 3. Results and discussion

Initially, we assumed the  $(N^1,N^1,N^2,N^2\text{-tetramethylethane-1,2-diamine})$  TMEDA role as a proton scavenger in the reaction of Scheme 2 and did not consider it as a ligand with CuCl in our computational study. We made the TMEDA-free assumption because Stack *et al.* reported the [(TMED)Cu(I)]<sup>1+</sup> complex instability in the presence of weakly coordinating anions and aprotic solvent.<sup>40</sup> As seen from the Gibbs energy profile, the **2CI-VD** formation is energetically "downhill" (Figure 1) in the case of the ligand-free (**LF**) route, which started with concerted transition state (**TS1-LF**,  $\Delta G^{\dagger}$ =17.3 kcal/mol) comprises Cl atom migration from CCl<sub>4</sub> to CuCl and the ·CCl<sub>3</sub> radical attack on the substrate. Considering that **I1-LF** intermediate contains CuCl<sub>2</sub>, we calculated both singlet and triplet state structures (**I1-LF-TRIP**) and

identified that the triplet state intermediate Gibbs energy is considerably higher (9.5 kcal/mol) compared to the singlet state. The next deprotonation step (TS2-LF) goes over a 10.7 kcal/mol energy barrier. The second chlorine atom removal (TS3-LF) from CCl<sub>3</sub>-substrate adduct (I2-LF-HCI) is calculated to have 5.9 kcal/mol energy, which results in I3-LF formation. Since I3-LF bears CuCl<sub>2</sub> its triplet version (I3-LF-TRIP) was also calculated to be 21.7 kcal/mol higher in energy than singlet state. We conclude that the singlet state intermediate (I3-LF) conversion via TS4-LF ( $\Delta G^{\ddagger}$ =11.3 kcal/mol) transition state results in the formation of product (2CI-VD). The overall reaction is calculated to be 33.0 kcal/mol exergonic in the case of the LF route. Our calculations revealed that the product formation is not a favorable path in the case of LF, since the TS4-LF energy is smaller than 2CI-VD.

Next, the reaction mechanism was examined with inclusion of one molecule of TMEDA as a ligand to CuCl to identify the CuCl complexation effect on the same reaction. Comparing to the **TS1-LF** energy barrier, the **TS1-L** ( $\Delta G^{\dagger}$ =25.6 kcal/mol) activation energy is calculated to be 8.3 kcal/mol higher. Previous experimental studies revealed that the obtained product (**2Cl-VD**) is in the trans configuration. Because of the **TS1-L** transformation probability to both the cis- (**I1-L-cis**) and the trans- (**I1-L-tns**) intermediates, we tested both routes shown in Figure 2.

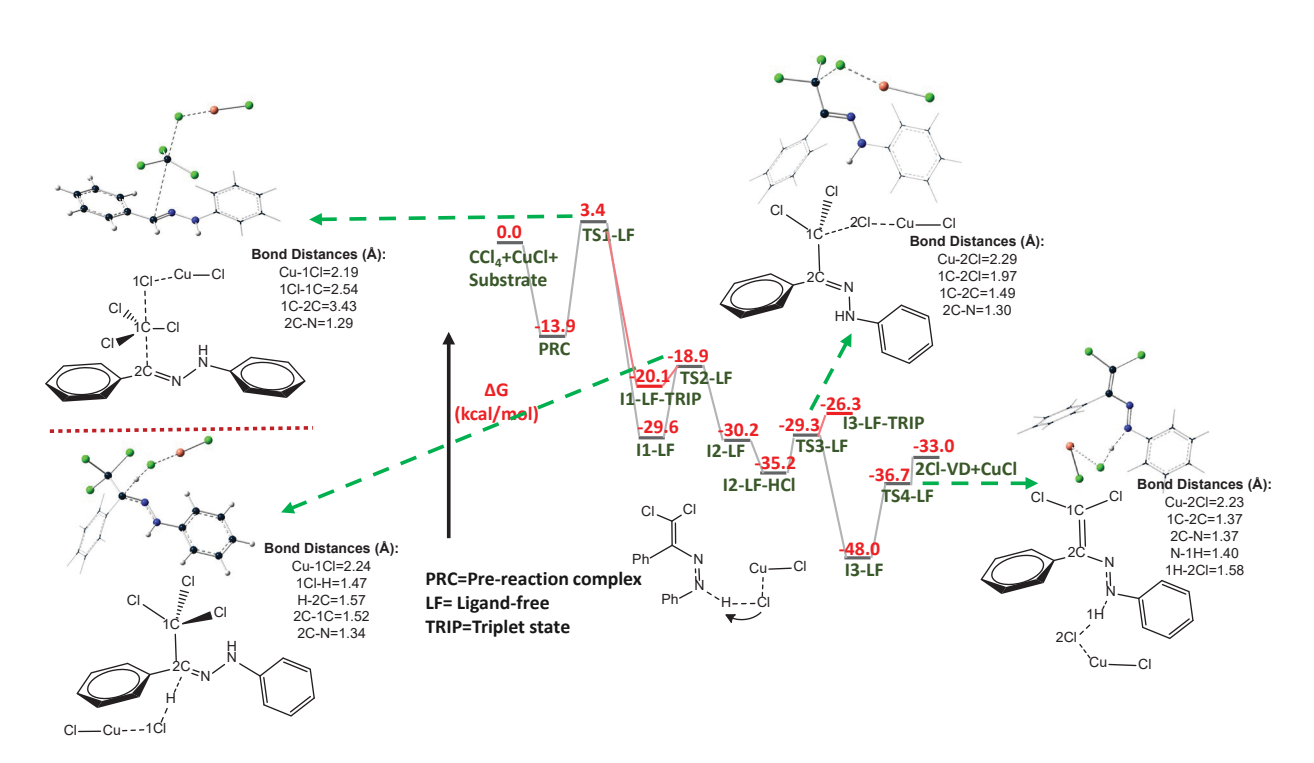


Figure 1. Gibbs free energy profile for  $CCl_4+CuCl+$  Ph-CH=N-NH-Ph (1-benzylidene-2-phenylhydrazine). Phenyl groups are omitted for the sake of clarity. All the species are optimized as singlet states, excluding species ending with TRIP. The Gibbs energy profile was designed based on the trans conformers.

The further deprotonation step in the case of trans route (**TS2-L-tns**, blue path in Figure 2) is calculated to have a 6.8 kcal/mol energy barrier. In comparison, the cis route energy barrier is much smaller (**TS2-L-cis**,  $\Delta G^{\ddagger}$ =2.2 kcal/mol, red path). The second chlorine atom removal energy barrier from the **I2-L-tns** intermediate is found to be 1.3 kcal/mol, whereas the cis analog (**I3-L-cis**) conversion is 5.8 kcal/mol higher in energy.

Both TSs (**TS3-L-tns** and **TS3-L-cis**, see Figure 3) can yield the trans structure since  $Cl_2C=C$  bond formation urges the structure to be more stable in the trans configuration. Because of the internal repulsive forces, the **TS3-L-cis** structure is 7.4 kcal/mol higher in energy than its trans analog. As seen in Figure 3, **TS3-L-cis**  $\rightarrow$  **I3-L-tns** conversion seems possible via the 2N-1N-2C-1C dihedral angle (DA) rotation. The phenyl hydrazone moiety of the **TS3-L-cis** is not on the same plane as the  $Cl_3C-C$ - part (DA=8.8°). A slight rotation toward the trans configuration indicates that the cis transition state (TS) structure is likely to produce a trans intermediate. Our computational findings are in good agreement with the X-ray analysis of the previously synthesized product structure. <sup>15</sup>

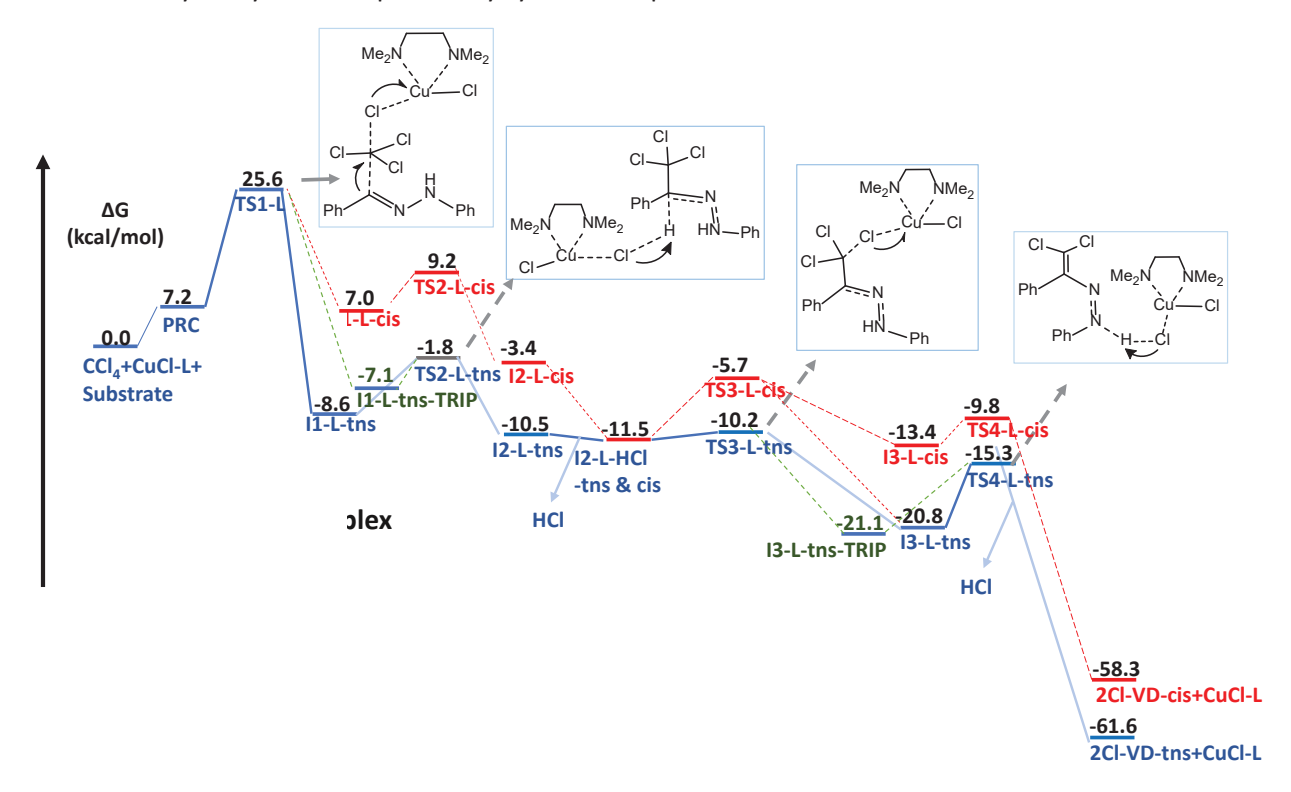
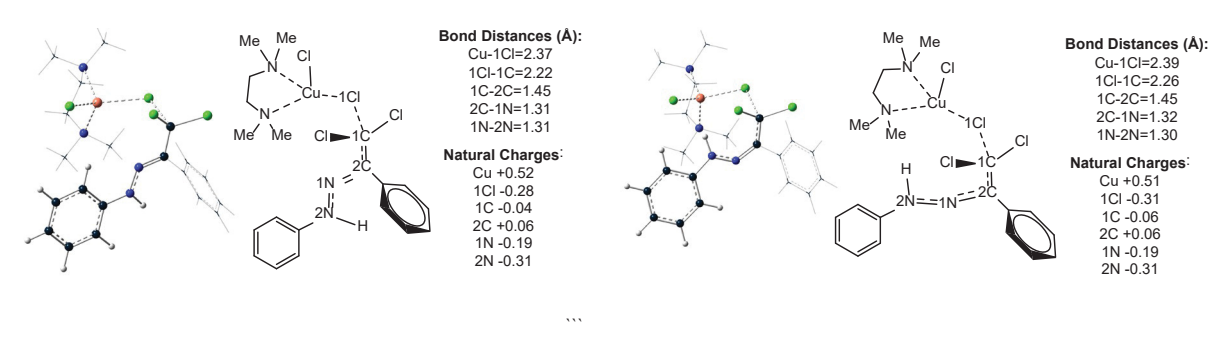


Figure 2. Gibbs free energy profile for CCl<sub>4</sub>+CuCl-L+ Ph-CH=N-NH-Ph. The blue route indicates the transformation of the starting compound to 2Cl-VD over trans and triplet state TSs and intermediates. The red route describes cis structures. All the species are optimized as singlet states, excluding species ending with TRIP.



**Figure 3**. Optimized structures of **TS3-L-tns** and **TS3-L-cis** with important bond lengths (given in Å) and natural charges. Hydrogen and carbon atoms of the aromatic ring and TMEDA are omitted for the sake of clarity.

We also conducted a Natural Bond Orbital (NBO) analysis<sup>41</sup> to examine the natural charges of selected atoms in the **TS3-L-tns** and **TS3-L-cis** structures. As seen in Figure 3, the differences in the atomic charges are small and unlikely to be associated with the selectivity of the reaction.

As seen in Figure 2, the more stable trans intermediates formation is also possible even though the reaction follows the cis route (red). **TS3-L-cis** and trans configurations result in the formation of **I3-L** intermediates via maintaining double bond 1C=2C (Figure 3). By 1C=2C formation the 1N-2C bond order becomes one, which supports free rotation through the 2N-1N-2C-1C DA. Because of the steric hinderance for the proton removal in the **TS4-L-cis** structure (See ESI, Figure S1), the reaction rather follows more stable trans route via rotation yielding the trans product. Compared to **TS3-L-cis**, in the **TS4-L-cis** structure the 2N-1N-2C-1C DA is expanded from 8.8° to 61.1°, which strongly supports our hypothesis. As a result of the TMEDA-CuCl complex and CCl<sub>2</sub> moiety repulsive interactions in the **TS4-L-cis** structure the rotation toward trans configuration becomes inevitable.

For better understanding of the TMEDA effects as a ligand on CuCl, we also conducted NBO analysis to compare the natural charges of Cu and Cl atoms in both CuCl and CuCl-TMEDA complex. In CuCl, the Cu charge is +0.78 e, which decreases to +0.54 e when CuCl forms complex with TMEDA. However, no significant differences in charge are noticed for the chlorine atoms (-0.78  $e \rightarrow$  -0.74 e). Considerable decrease in the copper natural charge indicates electron donation from TMEDA to Cu, resulting in lower electrostatic interaction between Cu and Cl atoms compared to CuCl. This provides the Cu atom in the CuCl-TMEDA complex with more availability to convert CuCl<sub>2</sub> by accepting an additional chlorine atom from CCl<sub>4</sub>, and other related species.

All the TS structures were optimized as spin singlets. Attempts to optimize them as spin triplet have failed due to convergence problems. This strongly supports the dominance of singlet states for the transition states. The chlorine atom removal form CCl<sub>4</sub> was conducted in two stages: PRC→I1-L-tns and I2-L-HCl→I3-L-tns both yielded CuCl<sub>2</sub> complex. As seen from Figure 1 and 2, most of the triplet state (I1-L-tns-TRIP, I1-LF-TRIP, and I3-LF-TRIP) intermediates have significantly higher Gibbs energies compared to the singlet state intermediates for the same step.

To validate the ligand-free CuCl and ligand-inclusive CuCl methodologies for the mechanistic studies we conducted additional calculations. Considering the possibility of CuCl dimer formation under the calculated reaction conditions (Scheme 2), we added one more CuCl molecule to the **TS1-LF** structure to re-optimize Cl removal from CCl<sub>4</sub> and  ${}^{\bullet}$ CCl<sub>3</sub> free-radical attack on the substate. The calculated energy barrier for the **TS1-LF+CuCl** is 16.1 kcal/mol, which represents a negligible change (1.2 kcal) compared to the same energy barrier for **TS1-LF**. Although we included the SCRF solvation model for DMSO in all our calculations to reflect solvent effect, we also modeled the possible CuCl-DMSO adduct synergetic effect on the reaction by adding one molecule DMSO to the **TS1-LF** structure. Our calculations demonstrated that the **TS1-LF+DMSO** energy barrier ( $\Delta G^{\ddagger}$ =19.7 kcal/mol) is slightly higher compared to that for **TS1-LF** (See ESI, Table S3 for energies and page S24 for xyz coordinates of the **TS1-LF+CuCl** and **TS1-LF-DMSO** structures).

Overall, for catalytic efficiency estimations, we used the energy span approximation using the Eyring equation <sup>42-44</sup> (See ESI). We calculated the turnover frequency (TOF) for the ligand included blue (trans) route in Figure 2 and compared the results with the ligand-free route. The ligand-included cis catalytic cycle infeasibility was scrutinized above. The fastest catalytic route (trans, blue) of Figure 2 was matched with the **LF** route described in Figure 1. Our observations revealed that in the **LF** case the TOF

(0.2) is considerably lower (the ligand-included blue route is faster by many orders of magnitude than the LF route), which suggests that TMEDA-Cu complex formation facilitates the substrates conversion to 2CI-VD. The amount of TMEDA was taken as 2.5 times than the main substrate concentration (See Scheme 2). One equivalent TMEDA, which possesses two tertiary amine groups, can neutralize HCl molecules released in the I1-L-tns→I2-L-HCl and I3-L-tns→2CI-VD steps. Computations suggest that complex formation (which speeds up the reaction according to TOF analysis) increases catalytic efficiency of CuCl on the tested reaction. Considering complex formation (with 1 mol% CuCl) and proton scavenging (using 1 eq TMEDA to neutralize 2 eq of HCl released from the reaction), 1.01 equivalents of TMEDA may be sufficient to conduct the reaction. The excessive TMEDA ligand utilization for the studied reaction may lead to additional complications by forming the [(TMEDA)₂Cu(I)]<sup>+</sup> complex, as previously suggested.<sup>40</sup>

#### Conclusion

The transformation of vinyldiazenes (**VD**) into diverse, value-added organic molecules under mild conditions has revealed the potential utilization of VDs in unexplored synthetic applications, solidifying their importance as fundamental building blocks in organic synthesis. Our primary focus was on the mechanistic studies of both the ligand-free (**LF**) and ligand-inclusive (**L**) pathways in the copper (I) chloride-catalyzed transformation of 1-benzylidene-2-phenylhydrazine and CCl<sub>4</sub> into (E)-1-(2,2-dichloro1-phenylvinyl)-2-phenyldiazene (2Cl-VD) to elucidate the role of copper (I) in the reaction. In comparison to the Cu-(I)-TMEDA complex, our calculations indicate that the **LF** route was the thermodynamically less favored pathway. Furthermore, our computational TOF analysis suggests that the inclusion of TMEDA significantly increases the rate of the reaction. Our computational analysis has indicated that using the less sterically hindered TMEDA ligand in complexation with CuCl enhances catalytic performance. This is achieved by reducing the energy barriers for chlorine removal steps, leading to faster product formation.

#### **Notes**

The authors declare no competing financial interest.

#### **CONFLICTS OF INTEREST**

There are no conflicts to declare.

#### **ACKNOWLEDGMENTS**

J.A. thanks The National Science Foundation, grant CHE-2152633, for support. All authors thank the Center for Computational Research (CCR, <a href="http://hdl.handle.net/10477/79221">http://hdl.handle.net/10477/79221</a>), University at Buffalo for providing computational resources.

### References

- 1. Attanasi, O. A.; Carvoli, G.; Filippone, P.; Perrulli, F. R.; Santeusanio, S.; Serri, A. M. Synlett 2004, 2004(09), 1643-1645.
- 2. Attanasi, O. A.; Berretta, S.; De Crescentini, L.; Favi, G.; Golobič, A.; Mantellini, F. Tetrahedron 2009, 65(11), 2290-2297.
- 3. Attanasi, O. A.; Favi, G.; Filippone, P.; Giorgi, G.; Lillini, S.; Mantellini, F.; Perrulli, F. R. Synlett 2006, 2006(17), 2731-2734.

- 4. Attanasi, O. A.; Favi, G.; Filippone, P.; Giorgi, G.; Mantellini, F.; Moscatelli, G.; Spinelli, D. Synfacts 2008, 2008(08), 0801-0801.
- 5. Attanasi, O. A.; Favi, G.; Filippone, P.; Mantellini, F.; Moscatelli, G.; Perrulli, F. R. Organic Letters 2010, 12(3), 468-471.
- 6. Boeckman, R. K.; Reed, J. E.; Ge, P. Organic Letters 2001, 3(23), 3651-3653.
- 7. Avalos, M.; Babiano, R.; Cintas, P.; Clemente, F. R.; Gordillo, R.; Jiménez, J. L.; Palacios, J. C.; Raithby, P. R. The Journal of Organic Chemistry 2000, 65(17), 5089-5097.
- 8. He, Z.-X.; Gong, Y.-P.; Zhang, X.; Ma, L.-Y.; Zhao, W. European Journal of Medicinal Chemistry 2021, 209, 112946.
- 9. Wermuth, C. G. MedChemComm 2011, 2(10), 935-941.
- 10. Asif, M. Journal of Chemistry 2014, 2014, 703238.
- 11. Bachollet, S. P. J. T.; Vece, V.; McCracken, A. N.; Finicle, B. T.; Selwan, E.; Ben Romdhane, N.; Dahal, A.; Ramirez, C.; Edinger, A. L.; Hanessian, S. ACS Medicinal Chemistry Letters 2020, 11(5), 686-690.
- 12. Aziz, S. I.; Anwar, H. F.; El-Apasery, M. A.; Elnagdi, M. H. Journal of Heterocyclic Chemistry 2007, 44(4), 877-881.
- 13. Sergeev, P. G.; Khrustalev, V. N.; Nenajdenko, V. G. European Journal of Organic Chemistry 2020, 2020(31), 4964-4971.
- 14. Attanasi, O. A.; Favi, G.; Filippone, P.; Perrulli, F. R.; Santeusanio, S. Organic Letters 2009, 11(2), 309-312.
- 15. Nenajdenko, V. G.; Shastin, A. V.; Gorbachev, V. M.; Shorunov, S. V.; Muzalevskiy, V. M.; Lukianova, A. I.; Dorovatovskii, P. V.; Khrustalev, V. N. ACS Catalysis 2017, 7(1), 205-209.
- 16. Sergeev, P. G.; Khrustalev, V. N.; Nenajdenko, V. G. European Journal of Organic Chemistry 2020, 2020(38), 6085-6093.
- 17. Shastin, A. V.; Tsyrenova, B. D.; Sergeev, P. G.; Roznyatovsky, V. A.; Smolyar, I. V.; Khrustalev, V. N.; Nenajdenko, V. G. Organic Letters 2018, 20(24), 7803-7806.
- 18. Abdullayev, Y.; Karimova, N.; Schenberg, L. A.; Ducati, L. C.; Autschbach, J. Physical Chemistry Chemical Physics 2023, 25(12), 8624-8630.
- 19. Xu, L.-P.; Li, N.; Musaev, D. G. Chemistry An Asian Journal 2023, 18(2), e202201145.
- 20. Schlegel, H. B. Journal of Computational Chemistry 2003, 24(12), 1514-1527.
- 21. Keith, J. A.; Vassilev-Galindo, V.; Cheng, B.; Chmiela, S.; Gastegger, M.; Müller, K.-R.; Tkatchenko, A. Chemical Reviews 2021, 121(16), 9816-9872.
- 22. Gurbanov, A. V.; Aliyeva, V. A.; Gomila, R. M.; Frontera, A.; Mahmudov, K. T.; Pombeiro, A. J. L. Crystal Growth & Design 2023, 23(10), 7335-7344.
- 23. Cui, H.; Xiao, D.; Zhang, L.; Ruan, H.; Fang, Y.; Zhao, Y.; Tan, G.; Zhao, L.; Frenking, G.; Driess, M.; Wang, X. Chemical Communications 2020, 56(14), 2167-2170.
- 24. Abdullayev, Y.; Rzayev, R.; Autschbach, J. Journal of Computational Chemistry 2022, 43(19), 1313-1319.
- 25. Khan, M. S.; Maha, N.; Riaz, M.; Yasmin, T.; Irfan, A.; Basra, M. A. R. Journal of Computational Chemistry 2023, n/a(n/a).
- Handley, D. A.; Hitchcock, P. B.; Lee, T. H.; Leigh, G. J. Inorganica Chimica Acta 2001, 316(1), 59-64.
- 27. Prescimone, A.; Sanchez-Benitez, J.; Kamenev, K. K.; Moggach, S. A.; Warren, J. E.; Lennie, A. R.; Murrie, M.; Parsons, S.; Brechin, E. K. Dalton Transactions 2010, 39(1), 113-123.
- 28. McCann, S. D.; Lumb, J.-P.; Arndtsen, B. A.; Stahl, S. S. ACS Central Science 2017, 3(4), 314-321.
- 29. Xu, B.; Hartigan, E. M.; Feula, G.; Huang, Z.; Lumb, J.-P.; Arndtsen, B. A. Angewandte Chemie International Edition 2016, 55(51), 15802-15806.
- 30. Xu, B.; Lumb, J.-P.; Arndtsen, B. A. Angewandte Chemie International Edition 2015, 54(14), 4208-4211.

- 31. Gessner, V. H.; Strohmann, C. Journal of the American Chemical Society 2008, 130(44), 14412-14413.
- 32. Frisch, M. J.; Trucks, G. W.; Schlegel, H. B.; Scuseria, G. E.; Robb, M. A.; Cheeseman, J. R.; Scalmani, G.; Barone, V.; Petersson, G. A.; Nakatsuji, H.; Li, X.; Caricato, M.; Marenich, A. V.; Bloino, J.; Janesko, B. G.; Gomperts, R.; Mennucci, B.; Hratchian, H. P.; Ortiz, J. V.; Izmaylov, A. F.; Sonnenberg, J. L.; Williams; Ding, F.; Lipparini, F.; Egidi, F.; Goings, J.; Peng, B.; Petrone, A.; Henderson, T.; Ranasinghe, D.; Zakrzewski, V. G.; Gao, J.; Rega, N.; Zheng, G.; Liang, W.; Hada, M.; Ehara, M.; Toyota, K.; Fukuda, R.; Hasegawa, J.; Ishida, M.; Nakajima, T.; Honda, Y.; Kitao, O.; Nakai, H.; Vreven, T.; Throssell, K.; Montgomery Jr., J. A.; Peralta, J. E.; Ogliaro, F.; Bearpark, M. J.; Heyd, J. J.; Brothers, E. N.; Kudin, K. N.; Staroverov, V. N.; Keith, T. A.; Kobayashi, R.; Normand, J.; Raghavachari, K.; Rendell, A. P.; Burant, J. C.; Iyengar, S. S.; Tomasi, J.; Cossi, M.; Millam, J. M.; Klene, M.; Adamo, C.; Cammi, R.; Ochterski, J. W.; Martin, R. L.; Morokuma, K.; Farkas, O.; Foresman, J. B.; Fox, D. J.; Gaussian Inc. Wallingford CT, 2016.
- 33. Hehre, W. J.; Ditchfield, R.; Pople, J. A. J Chem Phys 1972, 56(5), 2257-2261.
- 34. Grimme, S.; Antony, J.; Ehrlich, S.; Krieg, H. The Journal of Chemical Physics 2010, 132(15), 154104.
- 35. Pritchard, B. P.; Altarawy, D.; Didier, B.; Gibson, T. D.; Windus, T. L. Journal of Chemical Information and Modeling 2019, 59(11), 4814-4820.
- 36. Schuchardt, K. L.; Didier, B. T.; Elsethagen, T.; Sun, L.; Gurumoorthi, V.; Chase, J.; Li, J.; Windus, T. L. Journal of Chemical Information and Modeling 2007, 47(3), 1045-1052.
- 37. Aragoni, M. C.; Caltagirone, C.; Lippolis, V.; Podda, E.; Slawin, A. M. Z.; Woollins, J. D.; Pintus, A.; Arca, M. Inorganic Chemistry 2020, 59(23), 17385-17401.
- 38. Scalmani, G.; Frisch, M. J. The Journal of Chemical Physics 2010, 132(11), 114110.
- 39. Hratchian, H. P.; Schlegel, H. B. The Journal of Chemical Physics 2004, 120(21), 9918-9924.
- 40. Kang, P.; Bobyr, E.; Dustman, J.; Hodgson, K. O.; Hedman, B.; Solomon, E. I.; Stack, T. D. P. Inorganic Chemistry 2010, 49(23), 11030-11038.
- 41. Foster, J. P.; Weinhold, F. Journal of the American Chemical Society 1980, 102(24), 7211-7218.
- 42. Kozuch, S.; Shaik, S. Accounts of Chemical Research 2011, 44(2), 101-110.
- 43. Abdullayev, Y.; Abbasov, V.; Ducati, L. C.; Talybov, A.; Autschbach, J. ChemistryOpen 2016, 5(5), 460-469.
- 44. Abdullayev, Y.; Sudjaev, A.; Autschbach, J. Journal of Molecular Modeling 2019, 25(6), 173.